

C018

## Shallow Water CSEM Using a Surface-towed Source

D.V. Shantsev\* (EMGS), F. Roth (EMGS), C. Twarz (EMGS), A. Frisvoll (EMGS) & A.K. Nguyen (EMGS)

### SUMMARY

---

We address challenges for using controlled-source electromagnetic (CSEM) surveys at small water depths. A novel deployment setup where electrodes of a conventional CSEM source are suspended from two GPS positioned buoys and towed 10 m below the sea surface is proposed. This setup allows better control of the source position and orientation along with improved speed and manoeuvrability as demonstrated by a test survey in the North Sea. The finite-difference 3D modelling code used in data interpretation has been improved by a careful representation of source and receivers allowing an accurate modelling in shallow waters. Modelling results assuming a 2.2 km deep resistor demonstrate that a surface-towed source has essentially the same efficiency in detecting the target as the traditional deep-towed source if the water depth is within a few hundred meters. Additional attenuation of EM fields travelling through the water layer for surface-towing may be compensated by a better knowledge of these fields due to precise control of source position and orientation.

## Introduction

There is a growing interest for controlled source electromagnetic surveying (CSEM) for hydrocarbon exploration in marine environments at water depths of 100 m and shallower. Interpretation of CSEM data acquired in shallow water is challenging since the measured fields are dominated by an EM signal that has propagated along the air/water interface, requiring very accurate modelling and low overall data uncertainty. In addition, operational challenges exist in deploying a conventional source system designed for deep water acquisition.

In this abstract we present a shallow water deployment solution for a surface-towed source that has been tested recently and provides a number of advantages over a conventional deep-towed source. We then describe advances in our 3D finite-difference time domain (FDTD) modelling code needed to ensure accurate modelling results in shallow waters. In the last section, we analyze modelling results to demonstrate that a surface-towed source is equally efficient in detecting resistive targets as a deep-towed source in water depth of 100 m and even more.

## Surface-towed electric dipole source

Fig. 1 illustrates a shallow water deployment setup for surface towing of a conventional CSEM source (horizontal electric dipole). The electrodes of the source system are suspended from two GPS positioned buoys. The electrodes have negative buoyancy, ensuring constant depth below the buoys. A third float provides additional support for the towfish containing the current generator and for the umbilical. The float may also serve as a connection point for a towing cable.

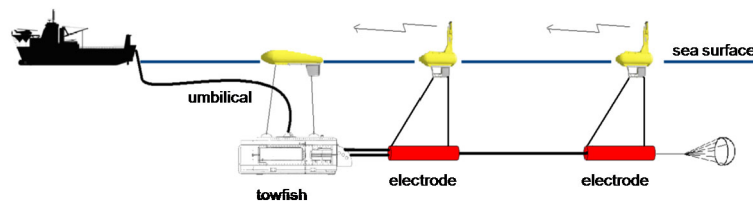


**Figure 1** Shallow water source deployment setup: The electric dipole source is suspended from GPS positioned buoys and towed at a constant depth below the sea surface.

The deployment setup has a number of benefits in terms of navigation accuracy, acquisition efficiency and safety:

- Accurate measurements of source position, length and feather angle due to high update dynamic GPS positioning of the electrode buoys
- Constant source depth (typically 10 m)
- Stable source pitch ( $< 0.1$  degrees)
- Possibility for fast towing (up to 4 knots)
- Improved source manoeuvrability leading to shorter tow line change times during 3D surveys
- No risk of impact with the seabed or subsea installations

Knowing the source position and orientation very accurately reduces the data uncertainty, which in turn allows for weaker CSEM responses to be measured, inverted and interpreted especially in shallow water environments. In addition, sagging and snaking usually shortens the actual source length by more than 10 m with respect to its nominal value. Hence exact knowledge of the electrode separation at all times allows for proper scaling of the data by the source dipole moment, thus reducing processing errors. For time lapse EM surveys, the constant source depth and source pitch provide improved source repeatability.

We conducted a surface towing test in the North Sea in 60-70 m deep waters (fig. 2a). The amplitude spectral density of the electric field recorded by one of the seabed receivers is shown in fig. 2b. The dominant harmonics of the source signal were at 0.125, 0.25, 0.375 and 1 Hz, and are clearly visible in the spectrogram. In addition, we observe a noise band centred at 0.08 Hz and related higher

harmonics during source passage as well as when the source is turned off. This frequency was equal to the main frequency of the measured vessel pitch and can hence be attributed to ocean swell, a common source of noise for EM measurements in shallow water. A way to mitigate ocean swell noise would be to analyse the frequency spectrum of the swell during deployment of the seabed receivers and then optimize the source waveform (Mittet and Schaug-Pettersen, 2008) to avoid overlap of transmitted signal with any observed noise frequency peaks. Even though no such waveform optimization was employed here, sufficiently low effective noise levels ( $10^{-15}$ - $10^{-14}$  V/Am<sup>2</sup>) were achieved for offsets up to 10 km except at the base frequency of 0.125 Hz.

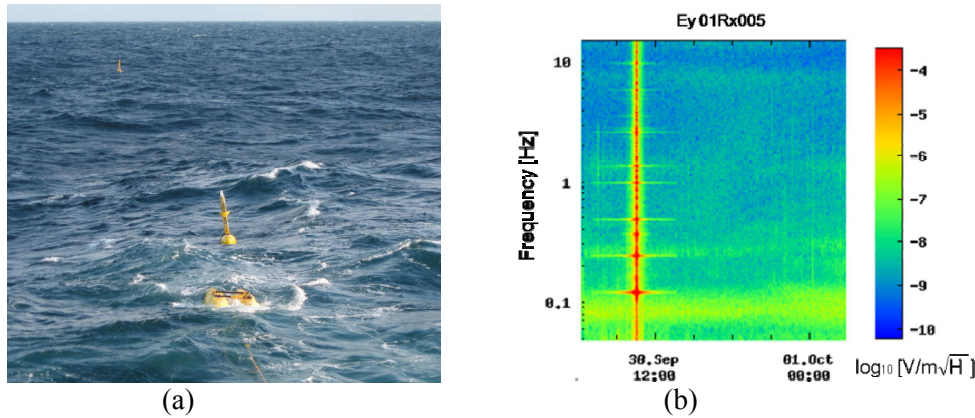


**Figure 2** Surface towing test with source at 10 m depth. (a) Photo showing the float supporting the towfish (front) and the two GPS positioned buoys from which the electrodes are suspended (back). (b) Example spectrogram of the electric field recorded on the seabed (water depth: 61 m).

### Accurate representation of sources and receivers in shallow water FDTD modelling

In this section we briefly review our 3D modelling code focusing on features that allow accurate modelling of a surface-towed source in shallow water. In finite-difference schemes, the nodes of the simulation grid do not necessarily coincide with the exact positions of the modelled sources and receivers. Therefore the modelled source should be properly distributed among adjacent grid nodes and the computed field values should be interpolated to the desired recording positions. In shallow water surveys, the source and the receivers are located very close to both the seabed and the sea surface. Both these interfaces are characterized by a strong conductivity contrast, which makes an accurate interpolation non-trivial. Below we focus on the horizontal components of electric and magnetic fields,  $E_x$ ,  $E_y$ ,  $H_x$  and  $H_y$ , which are most relevant for the shallow water case. Even though these field components are continuous across a horizontal interface, their vertical derivatives experience a discontinuity. The discontinuity can be ignored if one interpolates using only nodes in the water (Abubakar et al., 2008). The accuracy of such interpolation will however diminish as the water layer gets thinner. Instead, we suggest a rigorous interpolation method based on direct computation of the derivative jumps from Maxwell's equations and the known conductivity contrast at the interface. For example, the jump for  $H_y$  is estimated from the magnetic field curl equation,

$$\sigma_{xx}E_x = \frac{\partial H_z}{\partial y} - \frac{\partial H_y}{\partial z}, \quad (1)$$

where  $\sigma$  is the conductivity tensor and the source term is omitted since we consider fields close to a recording position. Since  $E_x$  and  $\partial H_z/\partial y$  are continuous across the interface, a jump in  $\sigma_{xx}$  must always be accompanied by a jump in  $\partial H_y/\partial z$ . Thus,

$$\frac{\partial H_{y1}}{\partial z} - \frac{\partial H_{y2}}{\partial z} = (\sigma_{xx2} - \sigma_{xx1})E_x, \quad (2)$$

where indices 1 and 2 correspond to the media above and below the interface, e.g., the water and the formation. Using similar analysis, one may compute the corresponding jumps in  $z$  derivatives of  $E_x$ ,  $E_y$  and  $H_x$ .

The computed derivative jumps are then included into a non-linear interpolation scheme based on Taylor expansion. It follows from Eq.2 that, to find  $H_y$  at an arbitrary receiver location, we should use

not only values of  $H_y$ , computed at the surrounding nodes, but also values of  $E_x$ . The latter will come with a weight proportional to the conductivity change at the interface. For a cubic Taylor expansion in 3 dimensions our interpolation will thus use  $4 \times 4 \times 4 = 64$   $H_y$  nodes and 64  $E_x$  nodes. Due to the reciprocity principle, similar formulas can be applied for interpolation of the source. For example, to model a magnetic dipole source in the  $y$ -direction, we place some source terms at the surrounding  $H_y$  nodes and some small “fictitious” source terms at  $E_x$  nodes. We have implemented the described interpolation scheme into a 3D FDTD code working in a modified wave domain (Maaø, 2007). The interaction of EM fields with air was implemented as an upward-continuation boundary condition based on a quasi-static approximation (Wang and Hohmann, 1993). For the modelling examples discussed in the next section, using a 40 m grid cell size, a simple trilinear interpolation led to  $\sim 1$ -2% error in the computed fields, which the present interpolation method was able to reduce to  $\sim 0.5$ -0.8%.

### 3D modelling results

The deployment solution for a surface-towed source described above offers a number of benefits due to better control of source position and orientation. At the same time the source is moved further away from potential resistive targets in the formation and from receivers at the seabed. Hence an important question is whether a surface-towed source would be less efficient in resolving resistive anomalies than a standard source towed close to the seafloor. The 3D modelling results presented in this section demonstrate that the shallow and deep sources have essentially the same efficiency in detecting resistors for shallow waters.

To illustrate this, we consider a target buried 2.2 km below the seafloor with lateral dimensions  $5 \times 3$  km<sup>2</sup> embedded in a homogenous formation. The resistivities of the seawater, formation and target are 0.3125, 2 and 100  $\Omega$ m, respectively. The target thickness is 50m, and the modelled receiver is placed above one of the target edges. Let us first consider 100 m water depth, see fig. 3 (left). We perform two simulation runs, one with and the other without the resistive target, and analyze the difference between the two computed fields – the so-called scattered field. The amplitude of the scattered inline electric field at 0.2 Hz scaled by the source dipole moment is shown on the top plot. First of all, we see that it is larger than the effective noise levels observed during the surface-towing test ( $10^{-15}$ - $10^{-14}$  V/Am<sup>2</sup>), implying that the target is detectable using CSEM. Interestingly, the scattered field depends non-monotonously on the offset with a dip around 2 km. This can be interpreted as a superposition of two physical processes: at short offsets the scattered field is mainly due to direct reflection of the EM field from the target, while at long offsets it is due to a partially guided field along the resistive layer.

The top plot actually shows two curves: one for a shallow source towed 10 m below the sea surface (red) and another for a deep source towed 30 m above the seabed (i.e. at 70 m depth). The curves are almost indistinguishable, indicating that both source configurations are equally efficient for resolving the resistive anomaly. This is to be expected since the difference in source depth, 60 m, is much smaller than the skin depth in water at 0.2 Hz, 629 m. The bottom plot shows the scattered field normalized to the background field (computed in the absence of the target). This normalized response displays a peak at  $\sim 5$  km offset, i.e. when the source and receiver are located above the opposite edges of the resistive target providing the optimal configuration for a partially guided EM field. The peak value which reaches 17-18% is again nearly identical for the shallow and deep sources. This conclusion holds true even for higher frequencies up to 1 Hz: the relative difference between the peak values remains below 10%.

The right half of fig. 3 shows similar results for relatively deep water, 500 m. Correspondingly, we compare here sources towed at 10 m and at 470 m depth. The target is still 2.2 km below the seafloor. The top plot shows that the scattered field for the shallow source is now noticeably smaller than for the deep one since the EM wave attenuates while travelling through additional 460 m of water. The difference however constitutes only  $\sim 20\%$  at 0.2 Hz. Moreover, the normalized scattered fields (bottom plot) have not changed much compared to the case of 100 m deep water. The peak value is still at  $\sim 18\%$ , and for offsets  $< 7$  km the shallow source provides even slightly larger normalized response. It opens up a possibility for using the surface-towed source in waters deeper than 100 m. When choosing the source type, one should however keep in mind that at higher frequencies the attenuation increases significantly, which is especially critical for the source towed near the surface.

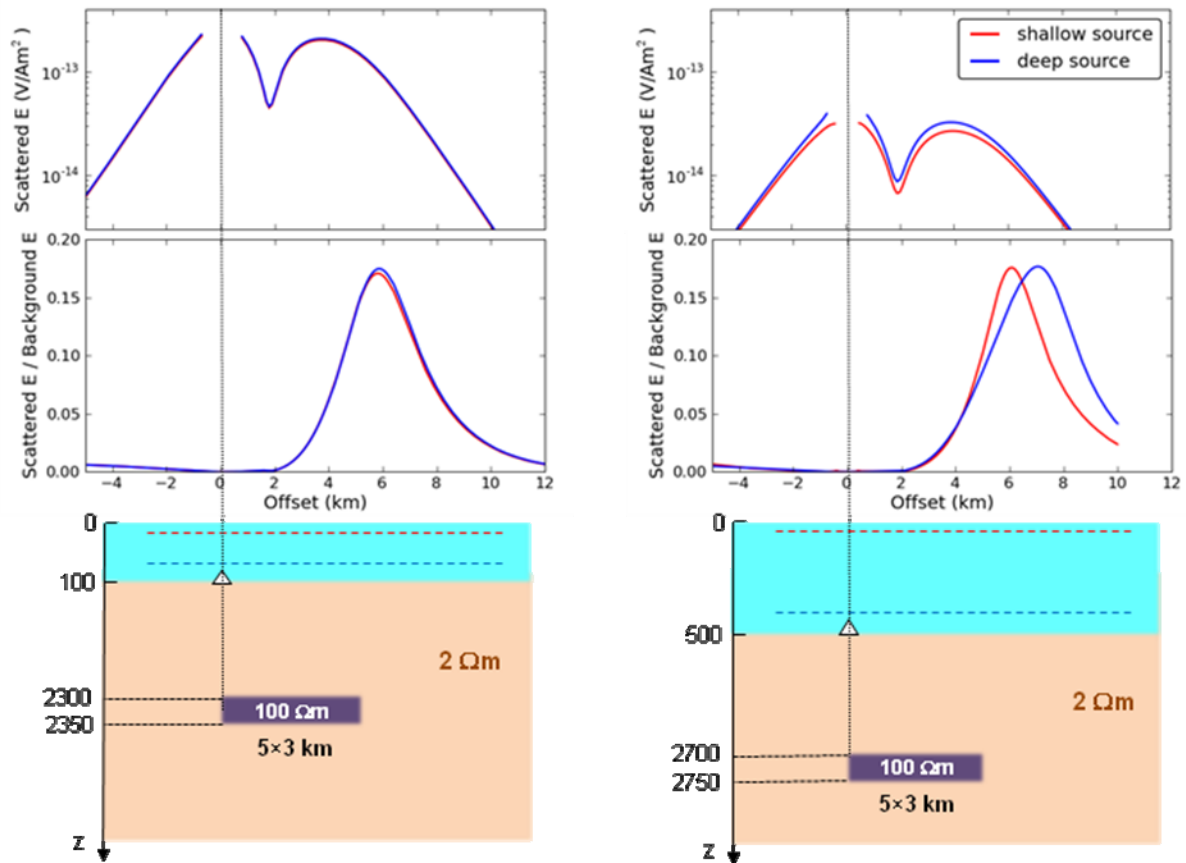


**Figure 3** FDTD modelling results for two sources: one towed at 10 m depth (red curves) and the other 30 m above the seabed (blue curves). Top: Amplitude of inline electric field scattered by the target at 0.2 Hz. Middle: Scattered field normalized to background field. Bottom: Sketch of the model. The shallow source produces equally strong responses for water depth of 100 m (left) and only slightly weaker responses for 500 m (right).

## Conclusions

We have presented a deployment setup for surface-towing a conventional CSEM source, and showed real and modelled data for such configuration. Surface-towing can be considered as an alternative to deep-towing in water depths of up to a few hundred meters. Additional attenuation of EM fields travelling through the water layer may be compensated by a better knowledge of these fields due to precise control of source position and orientation.

## Acknowledgements

We would like to thank EMGS for the permission to publish, Frank Maaø for proposing the advancements in our modelling and Jan Petter Morten for useful discussions. Thanks to Fugro Survey and Fugro Geoteam for providing some of the surface-towing equipment. Special thanks to the crew onboard BOA Thalassa that conducted the surface towing test with enthusiasm and professionalism.

## References

- Abubakar A., Habashy T. M., Druskin V. L., Knizhnerman L., and Alumbaugh D. [2008] *Geophysics* **73**(4), F165–F177.
- Maaø, F.A. [2007] Fast finite-difference time-domain modeling for marine-subsurface electromagnetic problems. *Geophysics*, **72**, A19–A23.
- Mittet, R. and Schaug-Petersen, T. [2008] Shaping optimal transmitter waveforms for marine CSEM surveys. *Geophysics*, **73**(3), F97–F104.
- Wang, T. and Hohmann, G.W. [1993] A finite-difference, time-domain solution for three dimensional electromagnetic modeling. *Geophysics*, **58**(6), 797-809.